Forest Chemicals Review
www.forestchemicalsreview.com
ISSN: 1520-0191
March-April 2022 Page No. 810-826
Article History: Received: 08 February 2022, Revised: 10 March 2022, Accepted: 02 April 2022, Publication: 30 April 2022

Outdoor and Contactless Body Size Measurement scheme through Multi-view Images for Full-size Animation Model Making under COVID-19

Chenxi Wang[1,2], Chang Ho Hong[1], Jinhua Xu[1], Xiyue Li[3], Zhenyu Wu[2], Xuanye Guo[2], Zhiwei Qiu[2,*], Zhijiu Han[1,4]

[1]Hanseo University, Haemi-myeon, South Korea
[2]School of Marine Technology and Geomatics, Jiangsu Ocean University, Lianyungang, China
[3]Pusan National University, Busandaehak-ro 63beon-gil, Geumjeong-gu, Busan, South Korea
[4]Chuzhou University, Chuzhou, China
*Corresponding author.

Abstract:

This paper focuses on the problem of human body size parameter measurement under the global novel corona virus (2019-nCoV) epidemic situation, and proposes a non-contact measurement scheme for human body with the principle of multi-view stereo vision. Furthermore, the motion recovery structure and multi-view dense reconstruction are used to extract the point cloud of human body. Based on the point clouds extracted, the size information of human body is obtained. As shown by the experimental results, compared with the traditional contact and other contactless measurements, this scheme has some advantages such as safety, low cost and wide range of application, which is a good supplement to the existing reconstruction technology. The reconstruction procedures of two kinds human bodies are analysed in this article. Some great advises have been concluded in this study through the different human bodies reconstruction errors analysis. Meanwhile, the results of automatic modelling can provide necessary materials for the animation model making in the next work.

Keywords: *Measurement of human body size, Multi-view Stereo, Structure from Motion, Animation model making.*

I. INTRODUCTION

Anthropometrics, as a crucial field in ergonomics, can determine the size difference between individuals and groups by measuring the size of multiple parts of the human body [1]. As the material level continues to improve, various parameters of the human body have become an important basis for the clothing design and health monitoring projects. Generally speaking, the measurement scheme of the dimension parameters of the human body can be classified into the “traditional contact measurement” and “non-contact measurement”.

Forest Chemicals Review
www.forestchemicalsreview.com
ISSN: 1520-0191
March-April 2022 Page No. 810-826
Article History: Received: 08 February 2022, Revised: 10 March 2022, Accepted: 02 April 2022, Publication: 30 April 2022

In terms of the traditional contact measurement, it is to obtain the size information of various parts of the human body through soft ruler and other equipment, which is both inefficient and tedious. Due to the extensive spread of the global novel coronavirus epidemic, it becomes particularly urgent to use the contactless human body size measurement scheme. Against this backdrop, the human body measurement scheme based on image processing and three-dimensional (3D) laser technology has become a safer choice [2]. Prior to the outbreak of epidemic, a lot of achievements have been made in the research of algorithms for extracting human body size parameters from 3D laser-point cloud data. For calculating the human body perimeter, Lu Guodong et al. [3] proposed the method of point cloud segmentation, grey detection, and minimum perimeter method. Apart from that, Chen Guoan et al. [4] adopted the fuzzy logic method to extract point cloud feature points and calculate human body size parameters.

In order to overcome the shortcomings of the above methods, based on the principles of multi-view stereoscopic vision, Schönberger J L and Frahm J M [5] applied Structure from Motion (SFM) algorithm and multi-view dense reconstruction algorithm. Furthermore, Multi-view Stereo (MVS) [6] was taken from common smartphone video to recover the 3D point clouds of the human body, and point cloud data was used to extract human body size parameters, according to GB/T 23698-2009 3D human body measurement standard issued by China in 2009 [7]. On this basis, the measurement results have been verified.

With the rapid development of deep learning, 3D reconstruction technology has also developed rapidly. Considering that traditional MVs is difficult to deal with weak texture areas, MVS algorithm based on deep learning came into being. More and more scholars began to study MVs algorithm based on deep learning. In recent years, many excellent network frameworks have emerged, such MVSNet[8], R-MVSNet[9], PointMVSNet[10], Cascade MVSNet[11], etc. Compared with the other three reconstruction networks, Cascade MVSNet adopts a cascade method, which can obtain high-resolution and accurate depth map without consuming too much GPU. Although the above researches have played very important role in the improvement of SFM three-dimensional reconstruction method, many algorithms are limited by equipment conditions and calculation cost, so they cannot carry out three-dimensional reconstruction and make original human body models quickly and cheaply under epidemic conditions. For the ordinary consumers without precision instrument, how to obtain their point cloud data and what is the accuracy of using ordinary camera, such as cell phone, to obtain human body 3D model based on SFM method become the interesting problems for our study.

II. METHODS

The measurement process of human body size is shown in Figure 1. Firstly, the multi-view image of the experimental object was collected and the feature points in the image were extracted. Secondly, SFM algorithm and MVS algorithm were used to obtain the sparse point cloud and dense point cloud data of human body. Furthermore, according to the scale parameters, this paper found the relevant feature points of the human body point cloud, and finally calculated the human body size parameters.

Forest Chemicals Review
www.forestchemicalsreview.com
ISSN: 1520-0191
March-April 2022 Page No. 810-826
Article History: Received: 08 February 2022, Revised: 10 March 2022, Accepted: 02 April 2022, Publication: 30 April 2022

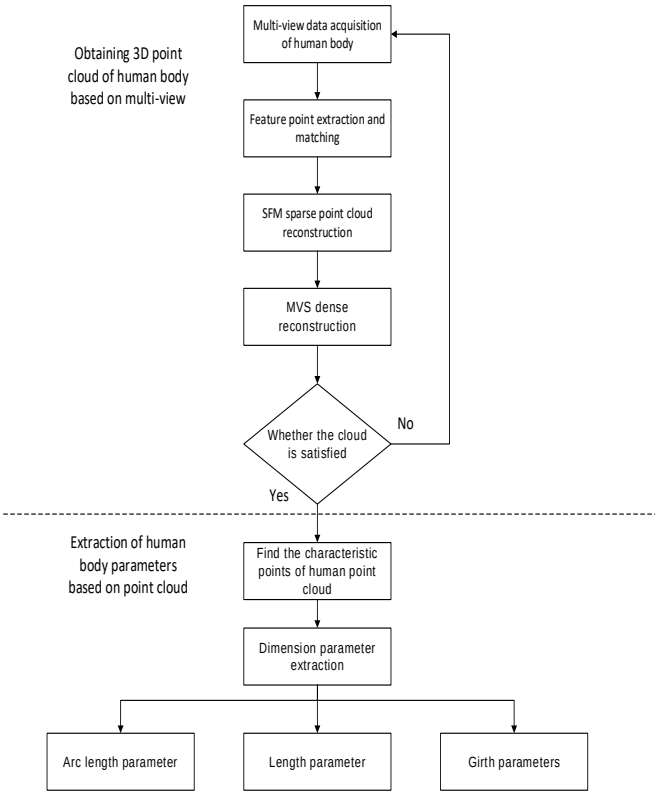

Figure.1: Flow chart of human body parameter extraction based on multi-view vision

In order to study the reconstruction precision of SFM 3D point cloud and grid model, the handheld digital camera is used to collect the image data of the target object under the condition of ensuring the consistent image overlap as far as possible. We collected the image data sets with different objects, including human bodies, and successively performed SFM sparse reconstruction, point cloud registration and grid reconstruction to obtain SFM 3D model, then quantitatively calculate the model reconstruction accuracy according with manual measurement, and analyzed the correlation between the reconstruction accuracy of SFM model and the reconstructed objects properties including texture, material and so on. The analysis of this experiment in our work also improves the three-dimensional human model reconstruction scheme based on SFM algorithm through normal dynamic video equipment.

III. HUMAN POINT CLOUD ACQUISITION BASED ON MULTI-VIEW STEREO VISION

After many years of development, the 3D reconstruction technology based on multi-view stereo vision has become increasingly mature. To be specific, it collects images from different angles of the reconstructed target, uses the texture features of the image to conduct stereo matching, and finally outputs the point cloud coordinate data of the target. This method, which is not limited by geometric information such as camera position and direction, only needs the image data with the reconstructed target. In the research, this method is used to reconstruct the point cloud data of human body, and the key steps are as follows:

Forest Chemicals Review
www.forestchemicalsreview.com
ISSN: 1520-0191
March-April 2022 Page No. 810-826
Article History: Received: 08 February 2022, Revised: 10 March 2022, Accepted: 02 April 2022, Publication: 30 April 2022

Step 1: Multi-perspective images acquisition. It is tedious to shoot multiple images around the human body. Thus, the reconstructed images can be obtained by shooting video and cutting the key frames. However, due to the volume of the body, after the experiment of many times, this research uses 90 best pictures about the effect of reconstruction and speed. It is assumed that video time is t, and the speed of the extraction photo is set to $\frac{t}{90}$.

Step 2: Image feature point extraction and matching. Specifically, 3D reconstruction is to restore the 3D coordinates of the target by different pictures of the same name point. Thus, the image feature point extraction and matching become increasingly important. Currently, the algorithm of feature point with Harris [11], oriented FAST and rotated BRIEF (ORB) [12] algorithm, Speeded Up Robust Features (SURF) [13-14] and Scale Invariant Feature Transform (SIFT) are popular. Given the robustness and speed of reconstruction, this paper uses the SIFT to complete the image feature point extraction.

SIFT is a feature point detection algorithm proposed by Lowe in 1999[9]. It not only calculates the position information of feature points (x, y) through Difference of Gaussian (DOG) filters of different sizes but also provides the descriptor information. The main steps of the SIFT algorithm are as follows: ① **Scale space extremum detection:** This research searches the image position on all scales, gets the scale space through the Gaussian differential function, and sets σ to represent the scale parameter. The scale space of the image $L(x, y, \sigma)$ can be expressed as:

$$L(x, y, \sigma) = G(x, y, \sigma) * I(x, y) \quad (1)$$

Where $I(x, y)$represents the input image, * represents the convolution symbol, $G(x, y, \sigma)$ represents the Two-dimensional Gaussian Kernel [10], and its expression is as follows:

$$G(x, y, \sigma) = \frac{1}{2\pi\sigma^2} e^{-(x^2+y^2)/2\alpha^2} \quad (2)$$

② **Location of the key points:** After the rough feature points of the image are screened out, some screening methods are used to eliminate the extreme points with low contrast, so as to improve the position accuracy of the key points in the image and the scale accuracy of the space.

③ **Determination of the direction of the feature point:** The feature vector has the coordinate value of the vector. Apart from that, it is essential to determine its direction parameters according to the gradient direction of its neighbourhood pixels. ④ **Generation of feature point descriptors:** This research takes each feature point as the centre and measures the local gradient of the graph at the selected scale in the neighbourhood around it, so as to produce feature points that allow scale and illumination changes.

After the positioning of the feature point is completed, the gradient of the point is calculated by using the 16 × 16 neighborhood of the feature point. Then, the 16 × 16 region is divided into 4 × 4 small areas, and the points of each region are projected in eight directions. A total of 128-dimensional feature vector

Forest Chemicals Review
www.forestchemicalsreview.com
ISSN: 1520-0191
March-April 2022 Page No. 810-826
Article History: Received: 08 February 2022, Revised: 10 March 2022, Accepted: 02 April 2022, Publication: 30 April 2022

descriptors has been obtained. In addition, the 128-dimensional feature descriptor is rotated to the principal direction, and the distance of the 128-dimensional feature descriptor is calculated.

Step 3: SFM sparse reconstruction. The input data of SFM algorithm are multiple images of the reconstructed target as well as the feature matching points obtained in the previous step. It is assumed that the projection of the object in the camera is shown in Figure 2.

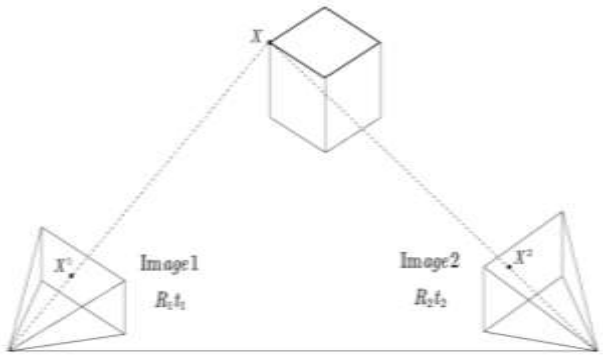

Figure.2: Schematic diagram of SFM

In computer vision, the spatial point $X(x, y, z)$ satisfies the spatial relationship with its projection point $X^1(u, v)$ in the image:

$$\begin{bmatrix} u \\ v \end{bmatrix} = K \times [R \quad t] \times \begin{bmatrix} x \\ y \\ z \end{bmatrix} = PX^1 \tag{3}$$

Where K is an internal parameter matrix and $[R \quad t]$ represents the image posture of the camera. According to the principle of antipolar geometry, the same point in the two images satisfies the functional relationship:

$$X^1 F X^2 = 0 \tag{4}$$

Where F refers to the basic matrix, and:

$$E = K_1^T F K_2 \tag{5}$$

According to the internal parameters of the camera, the essential matrix E can be obtained. Moreover, the three-dimensional coordinates of the points can be got by formula transformation. Then, more photos can be added to reconstruct the sparse point cloud data of the target.

In the process of continuously adding photos, errors will gradually accumulate, which can be reduced by Bundling Adjustment (BA) optimization [15]. BA optimization, as a widely used nonlinear optimization method, is derived from the formula of minimizing projection error:

$$\min_x \sum_i \rho_i \left(\| f_i(x_{i1}, x_{i2}, \ldots, x_{in}) \|^2 \right) \tag{6}$$

Where f_i represents the cost function, ρ_i represents the loss function, and x_{in} represents the parameter to be optimized.

Forest Chemicals Review
www.forestchemicalsreview.com
ISSN: 1520-0191
March-April 2022 Page No. 810-826
Article History: Received: 08 February 2022, Revised: 10 March 2022, Accepted: 02 April 2022, Publication: 30 April 2022

Step 4: MVS dense 3D Reconstruction. The sparse point cloud information, which is obtained by SFM algorithm, cannot reflect the precise geometric information of the target. The dense point cloud information of human body can be obtained by using MVS algorithm for dense reconstruction. In essence, the principle of MVS algorithm is the same as that of stereo vision. The sparse point cloud and camera pose output by SFM are used to gradually diffuse from feature points and judge whether the pixel points between images are the same. Finally, the dense point cloud of the whole target is reconstructed.

IV. BODY SIZE MEASUREMENT BASED ON POINT CLOUD DATA

After the acquisition and correction of the point cloud data of the target human body, the proportional coefficient between the actual height and the height in the model is firstly introduced. Then, the height of the point cloud model is calculated as the difference between the maximum and minimum point cloud coordinates in the direction of Y axis: $H = y_{max} - y_{min}$. After the model height is got, the proportion coefficient K is converted according to the actual height of human body.

The body size parameters extracted in this paper include height, shoulder width, arm, chest circumference, hip circumference, etc. In the process of dimension extraction, it is necessary to determine the position of relevant feature points of the human body, intercept the location plane of the feature points, and calculate the relevant dimensions. At the same time, there is a proportional relationship between the position of human feature points and height [16]. Assuming that the height of the feature points is H_x and the ratio between the height of the feature points and the height is λ_x, then the height of the human body feature points is $H_x = H \times \lambda_x$ (see Table I). According to the position of feature points, the section is obtained to calculate the size of each part.

Table I: PROPORTIONAL RELATIONSHIP BETWEEN POSITION AND HEIGHT OF HUMAN BODY FEATURE POINTS

Body feature points	The ratio of the position of feature points to the height of human body	
	male	female
The head point	1.00	1.00
The shoulder peak point	0.84	0.86
The point of chest height	0.72	0.72
Waist side point	0.61	0.63
The point of hip bumps	0.53	0.53
The knee point	0.26	0.28
The point of foot	0.00	0.00

Forest Chemicals Review
www.forestchemicalsreview.com
ISSN: 1520-0191
March-April 2022 Page No. 810-826
Article History: Received: 08 February 2022, Revised: 10 March 2022, Accepted: 02 April 2022, Publication: 30 April 2022

After feature point information related to the human body point cloud is obtained, the human measurement is classified as length, the circumference and the arc length according to different measurement requirements.

1) **Length**: The length size is composed of width, height, and linear distance. For width and height, its associated coordinate difference and the height $H_{ab} = y_a - y_b$ between AB are calculated. Regarding the straight line, according to the geometric distance formula, the straight-line distance (AB) can be calculated.

2) **Circumference**: Regarding the calculation of circumference, it is usually to find the feature point related to the measurement area. Moreover, the cross section of the feature point is adopted to intersect the human body point cloud to obtain a series of dot clouds, and solve the circumference of the point cloud.

3) **Arc length**: As for the calculation of arc length, a series of dot clouds are obtained based on the cross section of the measured area related feature point. Furthermore, the part and the arc length that is not related to the point cloud will be removed. Finally, the length of the lower cloud combined curve is the arc length.

V. EXPERIMENTS

5.1 Human body 1

In this study, the actual operating environment is Intel®Core™m3-6Y30, CPU0.90GHz, the internal storage is4GB, and the operating system is Ubuntu16.04. Apart from that, OpenMVG [17] and OpenMVS [18] libraries are used in an open-source frame. In the experiment, the ordinary smartphone is first used to collect human body video, and the body is surrounded by a circle, as shown in Figure 3 (a). Furthermore, the human body video of 44S is collected, and the OpenCV library is used to extract the photo, the first frame of the video and the last frame photos. Other extraction frequencies are 0.5s, and the specific shooting diagrams and extracted photos are shown in Figure 3 (b).

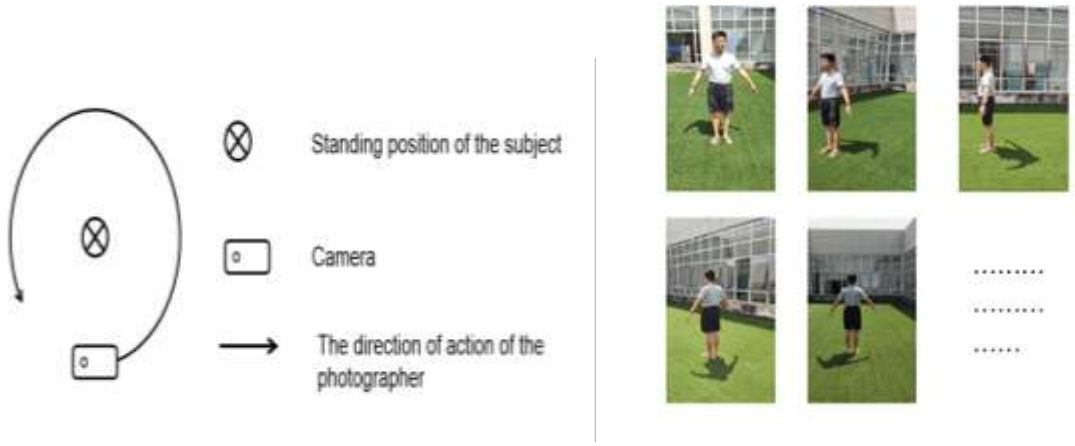

Figure. 3: (a) Geometric schematic diagram of captured video data, (b) Part of extracted pictures

Forest Chemicals Review
www.forestchemicalsreview.com
ISSN: 1520-0191
March-April 2022 Page No. 810-826
Article History: Received: 08 February 2022, Revised: 10 March 2022, Accepted: 02 April 2022, Publication: 30 April 2022

The SIFT algorithm is used to extract and match the feature points of two images with different viewing angles. Besides, 584 and 496 feature points are detected respectively in the two images. Then, the feature points are matched to a total of 286 homonym points (see Figure 4).

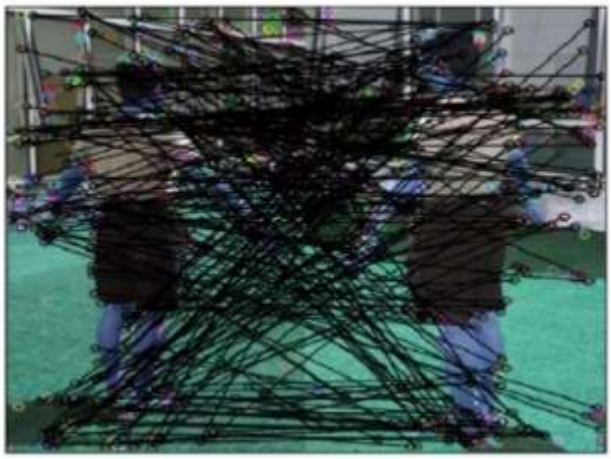

Figure.4: Matching results of SIFT feature points

Figure 5 is a point cloud and camera position using an SFM algorithm. Since the background other than the human body is not eliminated during the reconstruction, there are some noise points. After deletion of excess noise points, sparse Point Cloud is reconstructed. As displayed in Figure 6, the number of human body points reconstructed is 6,529, and the MVS algorithm is used to perform intensive reconstruction. Additionally, the dense thickening of the human body is obtained and shown in Fig. 7.

At the same time, the Poisson algorithm is used to reconstruct the thick point cloud, and the three-dimensional model obtained by the human body is displayed in Figure 8. Then, more steps can be performed.

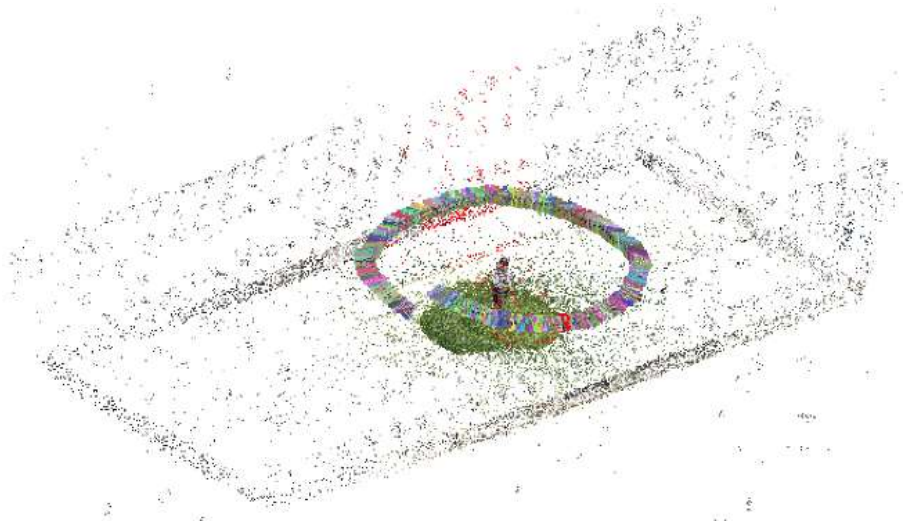

Figure.5: SFM reconstruction of point cloud and camera posture

Forest Chemicals Review
www.forestchemicalsreview.com
ISSN: 1520-0191
March-April 2022 Page No. 810-826
Article History: Received: 08 February 2022, Revised: 10 March 2022, Accepted: 02 April 2022, Publication: 30 April 2022

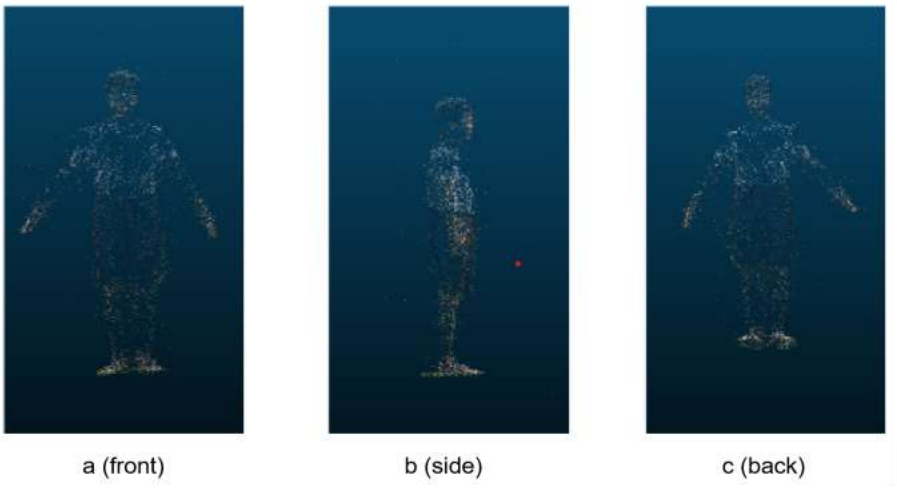

Figure.6: Sparse point cloud of human body

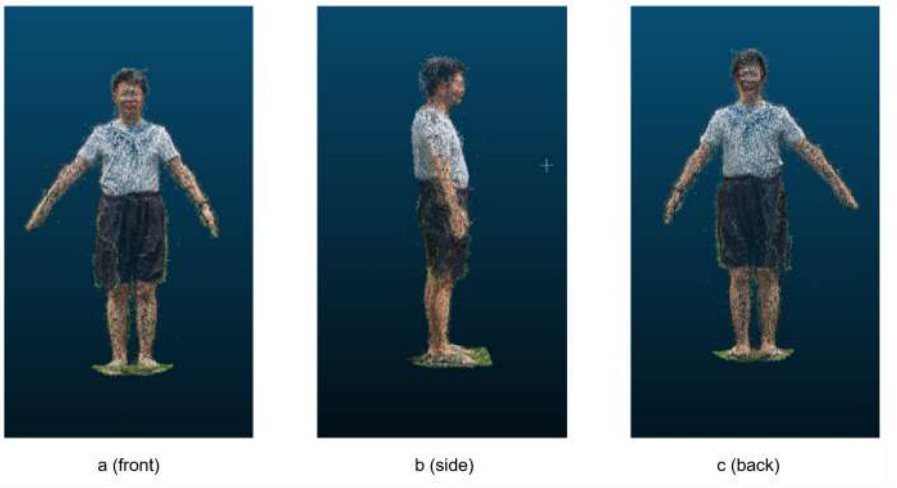

Figure.7: Dense point cloud of human body

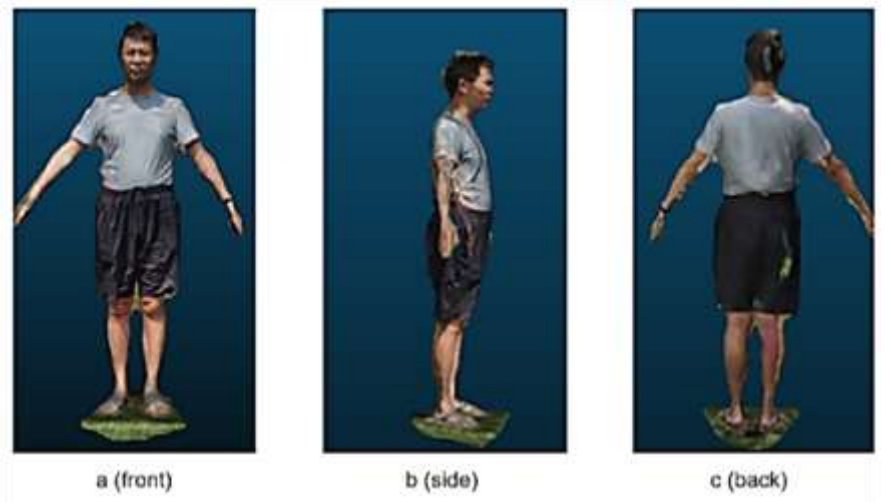

Figure.8: 3D reconstruced model of human body

Forest Chemicals Review
www.forestchemicalsreview.com
ISSN: 1520-0191
March-April 2022 Page No. 810-826
Article History: Received: 08 February 2022, Revised: 10 March 2022, Accepted: 02 April 2022, Publication: 30 April 2022

According to the human characteristics and height proportion, the coordinates of the relevant human body feature points are extracted by the proportional coefficient, the body size data is converted, and the function of the human body is measured to get the real size data of human body (see Table II). In this experiment, researcher collects three samples' data, where the maximum error is 1.40cm and the average error is 0.56cm. Furthermore, the above requirements in General Requirements for Anthropometric Methods of Three-dimensional Scanning [7] are compared. Overall, the experimental results have a certain value of use.

Table II: Comparison of measurement results (unit: cm)

Measuring site	Sample 1		Sample 2		Sample 3		Maximum error	Average error
	The scheme of this paper	Manual measurement	The scheme of this paper	Manual measurement	The scheme of this paper	Manual measurement		
Shoulder width	40.79	40.13	44.57	44.70	44.53	45.10	0.66	0.45
Chest girth	91.72	91.54	97.02	96.53	93.23	92.96	0.49	0.31
Arm length	55.02	54.40	59.48	59.70	56.32	55.90	0.62	0.42
Waistline	85.01	83.61	78.80	77.80	74.46	75.10	1.40	1.01
Hipline	88.41	89.26	98.16	99.12	95.30	95.23	0.96	0.63

5.2 Human body 2

In order to verify the robustness and effectiveness of the three-dimensional modeling method proposed in this paper, the second human body is reconstructed. Based on the above the SFM theory, the same method is utilized to reconstruct the second human body with more complex texture and shape compared with the first one shown in the Fig.9, so as to further explore the feasibility and accuracy of the research method in this paper. Because the same software and method as the three-dimensional reconstruction of the object above are used, the experimental process will not be redescribed in this section. Actually, the three-dimensional reconstruction method proposed in this paper does not depend on special instrument. In

Forest Chemicals Review
www.forestchemicalsreview.com
ISSN: 1520-0191
March-April 2022 Page No. 810-826
Article History: Received: 08 February 2022, Revised: 10 March 2022, Accepted: 02 April 2022, Publication: 30 April 2022

other words, Different and common dynamic video equipment also can be employed to collect the video data, such as our sell phone. The video data in this experiment is obtained through Mi 10 mobile phone, and its basic parameters are listed in Table III. As shown in the Fig.10, the sparse point cloud is reconstructed through Visual SFM software, and the generated sparse point cloud file bundle is displayed with the Meshlab software in fast way.

Table III: Dynamic video parameters of cell phone

Parameters	Value
Duration	0:00:28
Frame width	1920
Frame width	1080
Data rate	20016 kbps
Total bit rate	20210 kbps
Frame rate	29.76 frame/sec

Figure.9: Reconstruced target in the open field

Forest Chemicals Review
www.forestchemicalsreview.com
ISSN: 1520-0191
March-April 2022 Page No. 810-826
Article History: Received: 08 February 2022, Revised: 10 March 2022, Accepted: 02 April 2022, Publication: 30 April 2022

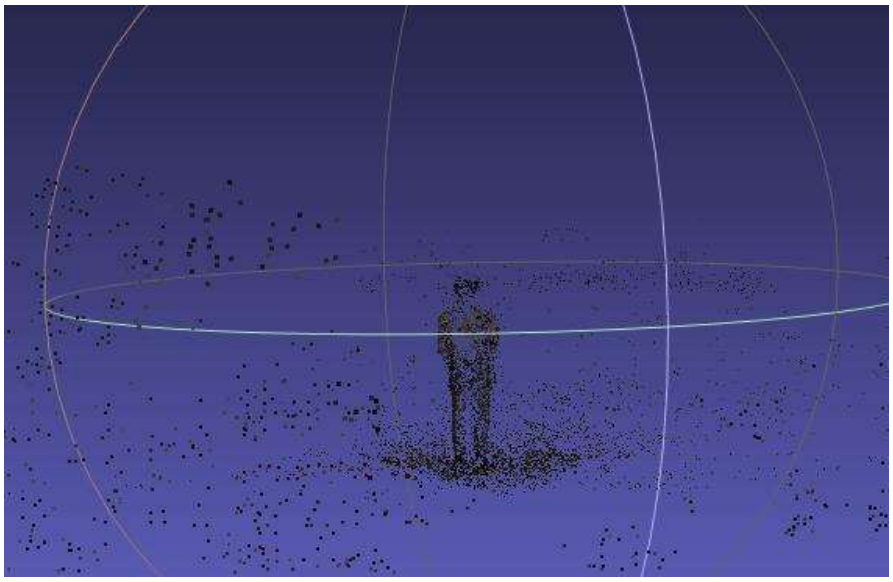

Figure.10: Sparse point cloud of human body

After the sparse point cloud generation, all photos are employed to reconstruct the dense point cloud, as shown in Figure 11. However, due to the redundant photos and the influence of the surrounding environment included the data source, there is a large amount of noise information in the reconstructed dense point cloud. Therefore, it is necessary to delete it and filter out the useless noise point cloud. As can be seen from Fig. 12, the 3D point cloud information of the human body can be basically preserved by automatically eliminating the noise point cloud through the threshold of parameters such as distance.

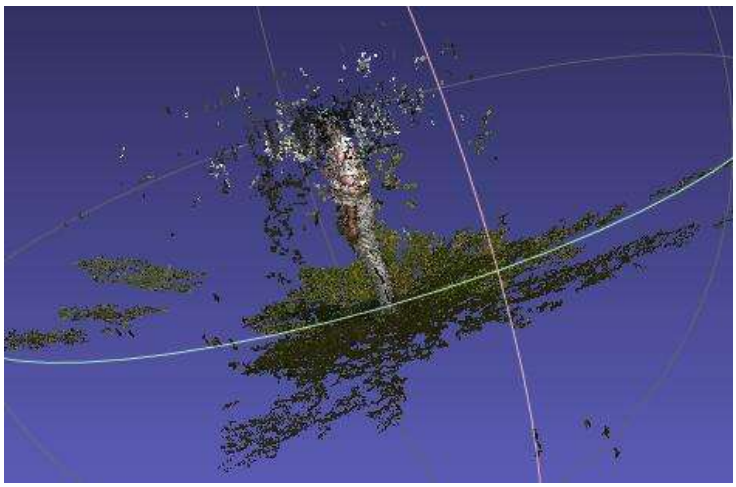

Figure.11: Dense point cloud of human body

Forest Chemicals Review
www.forestchemicalsreview.com
ISSN: 1520-0191
March-April 2022 Page No. 810-826
Article History: Received: 08 February 2022, Revised: 10 March 2022, Accepted: 02 April 2022, Publication: 30 April 2022

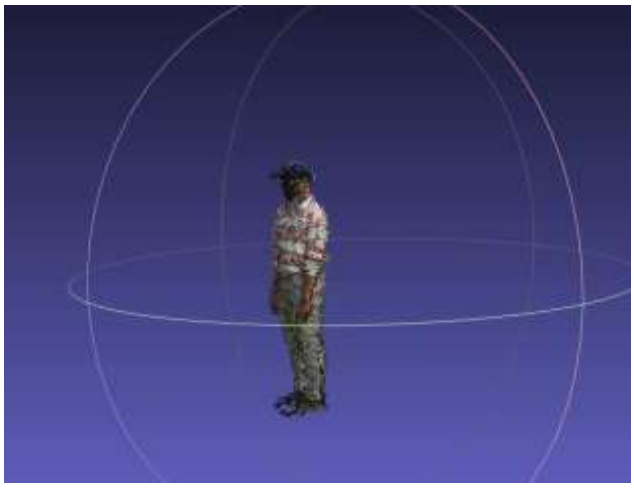

Figure.12: Filtered dense point cloud of human body

As mentioned above, Poisson Surface can be reconstructed after dense 3D point cloud data filtering. After the noise points filtered, the reconstructed surface illustrated in the Fig.13 looks very smooth and similar to the real human body. Due to more textures than the first human body, the final reconstructed 3D model through SFM algorithm can show us more details of the second human body in Fig. 14. Since the anthropometric points are extracted from the 3D human model with fixed height ratio illustrated in Table.1, the body dimensions gotten with such anthropometric points are not convincing enough which can affected by the manual measurement errors. Therefore, in this experiment of human body 2, as shown in Fig. 15, we adopted the direct verification method to acquire the model accuracy, that is, we calibrated the points of human shoulder width (M2), arm length (M1, M0) and leg length (M3, M4) on his real body and then calculated the difference with the corresponding points measured in the model. The impact of accidental error caused by height ratio can be reduce in this experiment

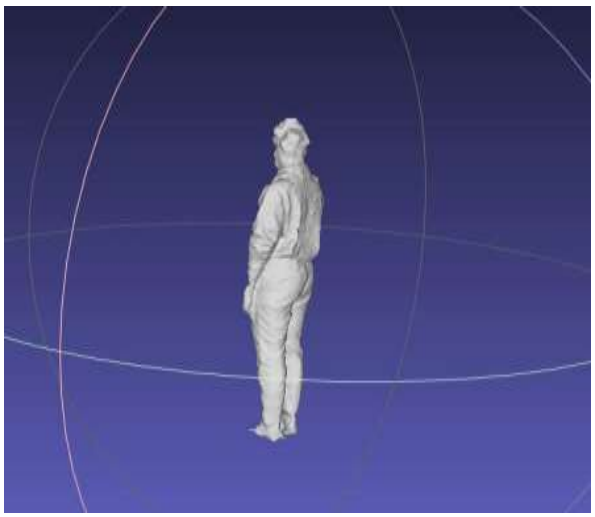

Figure.13: Poisson surface Reconstruction of human body

Forest Chemicals Review
www.forestchemicalsreview.com
ISSN: 1520-0191
March-April 2022 Page No. 810-826
Article History: Received: 08 February 2022, Revised: 10 March 2022, Accepted: 02 April 2022, Publication: 30 April 2022

Figure.14: Final 3D Reconstruction model of human body

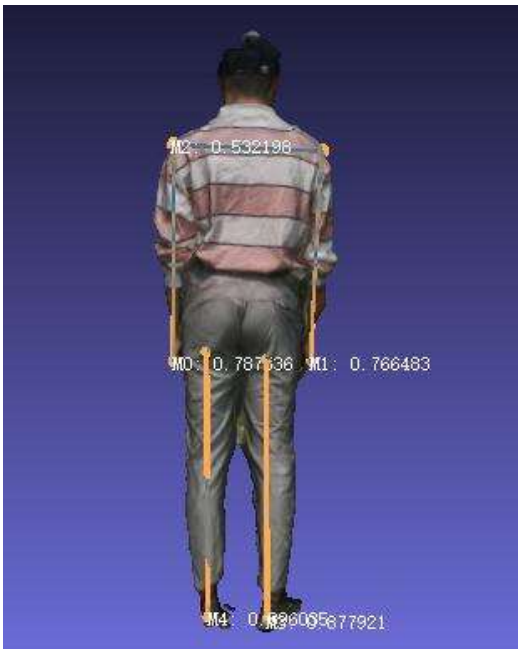

Figure.15: Human body model measurement

The measured line segments M0-M4 are shown in Figure 15, and the measured results are displayed around the dotted line. According to the unit of the software Meshlab, the measured data from the 3D model can be converted to compare with the direct measured data from the human body (we measured each length for five times and the average value could be calculated as the final results for verification). By comparing and analyzing these 5 model line segments measured by Meshlab software measurement tool and the manual measurements in the field, as shown in Table IV the mean error about 0.36 cm is more accurate than the first human body as we discussed above.

Forest Chemicals Review
www.forestchemicalsreview.com
ISSN: 1520-0191
March-April 2022 Page No. 810-826
Article History: Received: 08 February 2022, Revised: 10 March 2022, Accepted: 02 April 2022, Publication: 30 April 2022

Table IV: Measurement results of Human body model 2 (unit: cm)

Length name	Model measurements	Manual measurements	Bias
M0	78.75	78.63	0.12
M1	76.64	76.44	0.20
M2	53.21	52.47	0.74
M3	87.79	88.10	0.31
M4	89.60	90.03	0.43
Mean	-	-	0.36

VI. CONCLUSIONS

The human 3D model reconstruction experiments through dynamic video data based on SFM algorithm has been discussed in this paper. According to different measured verification methods, we mainly conducted 3D reconstruction for two human bodies. The first type of anthropomorphic measurement is to calibrate the positions of shoulder, waist and hip according to the proportion of human body, which is easy to operate and measure. However, due to the different features of each human body, it is easy to introduce the measurement errors. The second type of anthropomorphic measurement is the direct points calibration scheme on the human body, and makes full use of the clothes texture attached to the body, so as to better avoid accidental errors caused by field measurement. Through two human 3D reconstruction experiments, we can conclude that the main factors affecting the reconstruction errors are described as follow:

(1) Device quality: the higher the quality, the higher the accuracy. It is recommended to use dynamic video data acquisition tools with high pixel quality.

(2) Background light: the reconstruction accuracy of sufficient light parts is higher than the insufficient parts, such as the reconstructed chest of the human body is better than the head or the leg. It is recommended to acquire the video data in an environment with uniform light, and even appropriate lighting equipment can be considered.

(3) Noise reduction: The noise points filtering is needed and affects the dense point cloud reconstruction, resulting in slightly larger volume of 3 D model; It is recommended that manual elimination if this automatic filtering algorithm does not work well.

(4) Body posture: for example, the degree of joint bending can be changed dynamically during the measurement, so there are inevitable errors introduced in field data; it is recommended to remain as still as possible during video acquisition.

(5) Body clothing: The human body clothing with rich texture information is beneficial for 3D reconstruction and the more feature points can be obtained in the calculation. It is suggested that the reconstructed human body can be considered to wear the tight clothes with unified grid points.

Forest Chemicals Review
www.forestchemicalsreview.com
ISSN: 1520-0191
March-April 2022 Page No. 810-826
Article History: Received: 08 February 2022, Revised: 10 March 2022, Accepted: 02 April 2022, Publication: 30 April 2022

This paper not only uses the motion recovery structure in multi-view vision and MVS algorithm to reconstruct the 3D point cloud of human body, but also extracts the size parameters of human body from the point cloud. According to the experimental results, the reconstructed 3D point cloud of human body is effective, and the size parameters of the experimental target can be extracted from it. In short, it is a good supplement to the traditional non-contact measurement that uses 3D laser or depth camera to measure human body parameters.

To sum up, the 3D reconstruction technology based on SFM can rebuilt the full-size human 3D model under non-contact conditions and acquire the anthropometric data, However, in order to obtain reconstruction results with high precision, it is also necessary to consider the reconstruction procedures such as equipment, lighting, filtering, human posture and clothing, and even consider formulating some specifications in the collection process for the human body reconstruction, which will be our next work in the future.

STATEMENT

The collected human body images and data utilized in this article are voluntarily provided by the authors for reconstruction research. All the human participants declared that they provided the consent for their images and data to be published in the manuscript.

ACKNOWLEDGEMENTS

This work was supported by Scientific research project of Surveying and Mapping Geographic Information in Jiangsu Province [JSCHKY201904], in part by the Marine Technology Brand Major of Jiangsu Province [PPZY2015B116], and Jiangsu Ocean University’s 2020 Higher Education Teaching Reform Research Project [JGX2020006].

REFERENCES

[1] Xi Huanjiu & Chen Zhao (2010). The method of anthropometric measurement. Science Press.
[2] Lin Dejing & Sun Xiaodong (2005). Human body size extraction technology based on 3D scanning. Journal of Beijing Institute of Fashion Technology, 25(003), 36-41.
[3] Lu Guodong, Xu Peng & Xu Wenpeng. (2005). Research on feature extraction method of human body scanning model. Journal of Engineering Design, 12(4), 247-251.
[4] Chen Guoan, Liu Fei & Li Li. (2011). Feature size recognition and extraction of human point cloud using fuzzy rules. Journal of Computer Aided Design and Graphics, 23(008), 1393-1400.
[5] Schonberger, J.L., & Frahm, J.M. (2016). Structure-from-Motion Revisited. IEEE Conference on Computer Vision & Pattern Recognition (pp.4104-4113). IEEE.
[6] Harris, C., & M. Stephens. "A combined corner and edge detector." Alvey vision conference 1988.

Forest Chemicals Review
www.forestchemicalsreview.com
ISSN: 1520-0191
March-April 2022 Page No. 810-826
Article History: Received: 08 February 2022, Revised: 10 March 2022, Accepted: 02 April 2022, Publication: 30 April 2022

[7] National Ergonomics Standardization Technical Committee (2009).GB/T23698-2009. General Administration of Quality Supervision, Inspection and Quarantine of the People's Republic of China; China National Standardization Administration Committee.

[8] Yao Y, Luo Z, Li S, Fang T, Quan L. MVSNet: DepthInference for Unstructured Multi-View Stereo. In ECCV, 2018:767–783.

[9] Yao Y, Luo Z X, Li S W, et al. Recurrent MVSNet for high-resolution multi-view stereo depth inference//The IEEE Conference on Computer Vision and Pattern Recognition, 2019: 5525-5534.

[10] Chen R, Han S F, Xu J, et al. Point-based multi-view stereo network//IEEE International Conference on Computer Vision, 2019: 1538-1547.

[11] Gu X, Fan Z, Dai Z, et al. Cascade Cost Volume for High-Resolution Multi-View Stereo and Stereo Matching. 2020 IEEE, 2020:2492-2501.

[12] Rublee, E., Rabaud, V., Konolige, K., & Bradski, G. R. (2011). ORB: an efficient alternative to SIFT or SURF. IEEE International Conference on Computer Vision, ICCV 2011, Barcelona, Spain, November 6-13, 2011. IEEE.

[13] Rosten, E., & Drummond, T. (2005). Fusing points and lines for high performance tracking. Tenth IEEE International Conference on Computer Vision. IEEE.

[14] Furukawa, Y., and J. Ponce (2010). Accurate, Dense, and Robust Multiview Stereopsis. IEEE Transactions on Pattern Analysis and Machine Intelligence. 32.8(2010):p.1362-1376.

[15] Lowe, D. G. (1999). Object recognition from local scale-invariant features. Proc of IEEE International Conference on Computer Vision.

[16] Daniilidis, K., Maragos, P., & Paragios, N. (2010). [lecture notes in computer science] computer vision–eccv 2010 volume 6312//bundle adjustment in the large., 10.1007/978-3-642-15552-9(Chapter 3), 29-42.

[17] Moulon, P., Monasse, P., Perrot, R, & Marlet, R. (2017). OpenMVG: Open Multiple View Geometry. International Workshop on Reproducible Research in Pattern Recognition. Springer, Cham.

[18] Shen, S. (2013). Accurate multiple view 3d reconstruction using patch-based stereo for large-scale scenes. IEEE Transactions on Image Processing, 22(5).